Earthquake Geotechnical Engineering for Protection and Development of Environment and Constructions – Silvestri & Moraci (Eds)
© 2019 Associazione Geotecnica Italiana, Rome, Italy, ISBN 978-0-367-14328-2

Site response analyses for seismic microzonation: Case-histories, results and applications in Central Italy

A. Pagliaroli
Dipartimento di Ingegneria e Geologia, Università degli Studi "G. d'Annunzio" di Chieti Pescara, Italy

I. Gaudiosi, R. Razzano, S. Giallini, F. de Silva & A. Chiaradonna
Istituto di Geologia Ambientale e Geoingegneria, CNR, Roma, Italy

A. Ciancimino & S. Foti
Politecnico di Torino, Italy

ABSTRACT: The paper presents the main results of 1D/2D site response numerical analyses at 4 sites selected among the 137 municipalities of the Seismic Microzonation study which has been carried out after the 2016 Central Italy seismic sequence. Complex site effects at ridge/slope crest and at the edge of slope covers lead to 2D aggravation factors in the range 2-3 with respect to ground motion predicted with simple 1D analyses. A systematic comparison carried out for all 137 municipalities, between computed and Italian code NTC18 amplification factors highlighted that the code is generally conservative at low-to-medium periods and over-conservative at medium-to-high periods. A strategy for the use of microzonation site response analyses in support of seismic design for the reconstruction process is finally suggested.

1 INTRODUCTION

The Italian guidelines (Working Group ICMS, 2008) for Seismic Microzonation studies propose three different stages: level 1 is a qualitative study based on geological information; level 2 is based on calculation of site amplification from standard charts; level 3, hereafter SM3, is based on quantitative assessment of site effects by means of site response numerical analyses. SM3 studies were carried out for the reconstruction of 137 municipalities in Central Italy which have been struck by the 2016 seismic sequence started with the Mw 6.0 earthquake on August 24, 2016, followed by the Mw 5.9 on 26 October and the Mw 6.5 on 30 October events (Chiaraluce et al., 2017). The studies were carried on by professionals (mainly geologist and geotechnical engineers) with the scientific supervision and support of the Center for Seismic Microzonation and its applications (CentroMS, https://www.centromicrozonazionesismica.it/en/) constituted by several universities and research institutes.

In the paper the results of site response numerical analyses carried out at 4 selected sites characterized by complex morphological and geological conditions are reported. Specifically, as shown in Figure 1, three sites are in the Marche Region (Arquata del Tronto, Monte San Martino and Montedinove), one in the Lazio Region (Saletta). The main features of the selected sites are briefly summarized hereafter (see Figure 1): 1) Monte San Martino lies on a structurally asymmetric gentle hill characterized by an outcropping seismic bedrock on one side and soft eluvio-colluvial covers on the other flank; 2) Arquata del Tronto is located at the top of a ridge characterized by the alternation of different rock lithotypes, weathered and jointed in the upper portion; 3) Montedinove site represents a symmetrical ridge situation characterized by the presence of an inversion in the shear wave velocity (V_S) profile; 4) Saletta is located on a depositional sandy terrace resting on an asymmetric rock ridge.

In the framework of the seismic microzonation project, in situ tests were carried out including down-hole (DH), Multichannel Analysis of Surface Waves (MASW), and Horizontal to Vertical

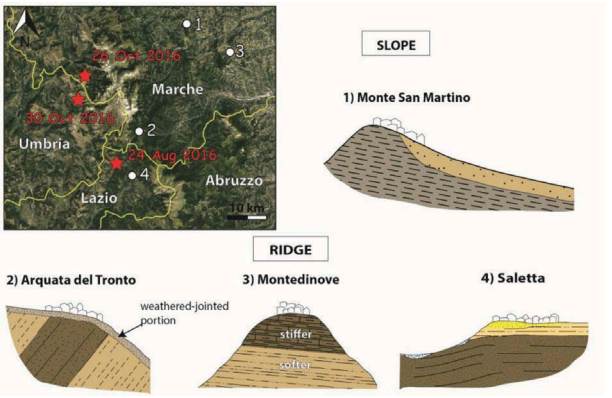

Figure 1. Sites considered and sketch of the corresponding geological/morphological configurations.

Spectral Ratios (HVSR) tests (Caielli et al., 2019). In some sites, other in situ tests were also available from previous studies such as Electrical Resistivity Tomography (ERT), P-wave seismic refraction (SR), Refraction Microtremor (REMI) and Extended Spatial Autocorrelation (ESAC) passive tests. On sites where it was possible to retrieve undisturbed samples, resonant column (RC)/torsional shear (TS) tests were also carried out (Ciancimino et al., 2019).

The 1D numerical analyses have been performed using STRATA (Kottke and Rathje, 2013) except for Montedinove case for which Deepsoil v 6.1 (Hashash et al., 2016) has been employed. Frequency domain analyses using the equivalent-linear visco-elastic approach were executed with both codes. The 2D analyses were carried out through the time domain 2D FEM codes LSR2D (Stacec 2017) for Montedinove case study and QUAD4M (Hudson et al., 1994), for Monte San Martino, Arquata del Tronto and Saletta. Both 2D codes adopt an equivalent-linear visco-elastic approach and incorporate a compliant base.

In all sites the input motions consisted of seven unscaled horizontal records selected by the ITACA archive (itaca.mi.ingv.it/), selected to be compatible on average, in the 0.1-1.1 s period range, with the Uniform Hazard Spectrum (return period T_R = 475 yrs) at flat outcropping rock conditions, i.e. subsoil class A – topographic category T1 as proposed by the Italian Building Code NTC18 (Ministry of Infrastructure and Transportation, 2018). More details on the procedure followed for the definition of input motion are reported in Luzi et al. (2019).

Results of numerical analyses have been processed in terms of elastic acceleration response spectra (Sa) and amplification factors of spectral acceleration (AF); these parameters have been assigned to each microzone of the level 3 seismic microzonation map (Pergalani et al., 2019). The AFs are defined as the ratio between the 5% damped elastic average acceleration response spectra at ground surface and the corresponding input spectra integrated over three period ranges 0.1-0.5s, 0.4-0.8s and 0.7-1.1s, labelled $AF_{0.1\text{-}0.5}$, $AF_{0.4\text{-}0.8}$ and $AF_{0.7\text{-}1.1}$ respectively. Moreover, 2D/1D aggravation factors (Pitilakis et al., 2015; Madiai et al., 2017) were computed at selected points to highlight the 2D effects in complex conditions. The values of aggravation factors are not significantly affected by the different employed computer codes considering that: i) both 1D and 2D simulations adopt the equivalent linear approach, ii) LSR2D-QUAD4M use the 2 control frequencies full Rayleigh formulation which provides results comparable to the frequency independent damping scheme adopted by the 1D codes (Lanzo et al., 2003).

In the following, for each case study the main morphological and geological features, the subsoil model and the results of the numerical analyses are summarized. At each site, response spectra and amplification factors calculated from numerical analyses are then compared with the corresponding parameters derived from the standard spectra of the simplified approach proposed by the Italian code NTC18. Differences are discussed also in the light of a statistical analyses carried out on all 137 municipalities subjected to SM3 studies. Finally, criteria for the use of SM3 studies in defining the design seismic actions for the reconstruction process, proposed by Presidency of the Council of Ministers (2018) are briefly presented.

2 CASE-HISTORIES

2.1 *Monte San Martino*

Monte San Martino is a small village in the Marche region, located about 30 km south of Macerata. The city centre lies on top of a rocky hill at 603 m a.s.l. between two deep valleys that separate Monte San Martino from the neighbouring municipalities located on the top of the surrounding hills.

Figure 2a shows the lithotechnical map of the area, with the location of in-situ investigations and the trace of a representative cross-section oriented in the WSW-ENE direction. The related cross-section is reported in Figure 2b, in which several lithotypes can be identified. The Blue Clays Formation (FAA in Figure 2) widely outcrops in the studied area. This formation can be subdivided in different lithotypes: the FAA-LPS consisting of mainly arenaceous lithofacies, i.e. alternations of thick arenaceous layers, locally cemented, and thin pelitic layers (1-3 cm), largely outcropping in the study area; the FAA-ALS formation consisting of arenaceous-pelitic lithofacies with sand/clay ratio higher than one, characterized by alternations of arenaceous and pelitic layers between 30 and 50 cm thick; the FAA-COS constituted by blue-grey clay with interleaved sandy horizons. Below the Blue Clays Formation, the geological bedrock is constituted of pelitic-arenaceous lithofacies with sand/clay ratio lower than one, recognized as "Colombacci" formation (FCO-ALS in Figure 2b). Eluvio-colluvial deposits (ML), constituted by clayey silt and silty sand, locally including arenaceous clasts, cover FAA in the eastern flank. Finally, at the top of the hill, a landfill material in a silty-sandy matrix (RI) has been recognized.

Table 1. Monte San Martino site: subsoil model for site response analyses (TS=Torsional Shear)

Lithotype	γ (kN/m^3)	V_S (m/s)	ν (-)	Nonlinear material curves
ML	20.0	220	0.48	TS test Monte San Martino
FAA-COS	22.5	450	0.45	
FAA-ALS upper	22.5	457	0.47	TS test
FAA-ALS lower	22.5	630	0.47	Massa Fermana
FCO-ALS upper	22.5	440	0.45	
FCO-ALS lower (bedrock)	22.5	800	0.45	Linear D=0.5%
FAA – LPS (bedrock)	24.0	800	0.45	Linear D=0.5%

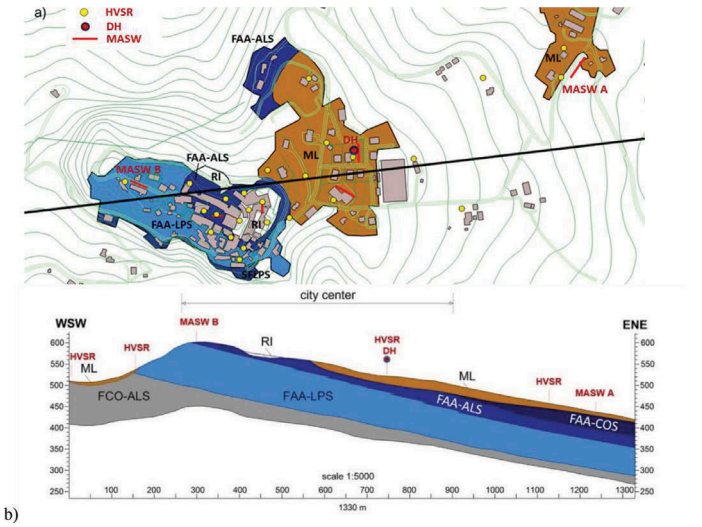

Figure 2. Monte San Martino lithotechnical map (a) and analyzed cross-section (b); lithotype codes are chosen according to the Italian standards for Seismic Microzonation (Working Group ICMS, 2008)

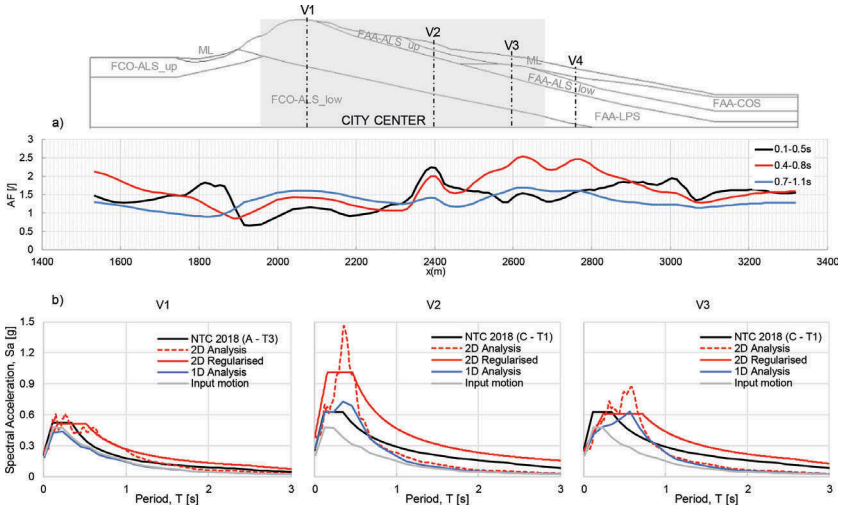

Figure 3. Monte San Martino site: a) profile of amplification Factors (AF) computed in the three period ranges T = 0.1-0.5s, 0.4-0.8s, 0.7-1.1s; b) average response spectra (ξ=5%) at V1, V2 and V3 computed through 2D and 1D numerical analyses compared with NTC18 spectra from simplified approach.

Table 1 summarizes the physical and mechanical properties assigned to the layers based on available geophysical tests (DH, MASW A and MASW B in Figure 2) or measurements carried out in nearby sites. Overall, the low-strain parameters of the model, as well as the bedrock depth, were validated by comparing the experimental predominant frequencies from HVSR curves with the resonance frequencies computed through 1D seismic response analyses at the same points (Pagliaroli et al., 2019a).

Figure 3a shows the variability along the cross-section surface of the mean amplification factors of the spectral acceleration computed with 2D analyses in the period ranges 0.1-0.5s, 0.4-0.8s and 0.7-1.1s. The highest AFs occur on the slope (i.e., eastern flank of the ridge) at the eluvio-colluvial deposit ML, with peak mean values $AF_{0.1\text{-}0.5}$ =2.23, $AF_{0.4\text{-}0.8}$ =2.50 and $AF_{0.7\text{-}1.1}$ =1.70. Lower amplifications, related to the topography, characterize the top of the ridge (mean values $AF_{0.1\text{-}0.5}$=1.13, $AF_{0.4\text{-}0.8}$=1.40 and $AF_{0.7\text{-}1.1}$=1.59); they exceed at medium-to-high periods the simplified topographic amplification factor (1.2) proposed by NTC18 or Eurocode 8 (CEN, 2004) for the corresponding topographic category.

To isolate and quantify the stratigraphic amplification, one-dimensional seismic response analyses have been carried out along representative soil columns, identified by verticals V1, V2, V3 and V4 on the cross section in Figure 3a. The 1D simulations were performed considering the same soil properties of 2D analyses. Response spectra from 1D and 2D analyses are reported in Figure 3b and compared with average input spectra at representative points V1 (crest) and V2, V3 (slope). With reference to the vertical V1, at the top of the ridge, as said before, amplification is exclusively due to topographic effects revealed by 2D analysis (1D spectrum obviously match the input one). At V2, located on the slope where soil cover outcrops, 1D and 2D computations lead approximately to the same spectral accelerations for T > 0.5s while significant 2D effects, probably related to buried morphology (V2 is located close to the edge of ML layer), appear at lower periods. Minor 2D effects take place at V3 (see 1D and 2D spectra in Figure 3b) where ground motion amplification is therefore mainly due to stratigraphic effects which are well-predicted by 1D seismic response analysis (the same behavior was found at V4, see also Pagliaroli et al., 2019a). In Figure 3b the 2D spectra regularized according to the procedure proposed in Working Group ICMS (2008) and the spectra computed by means of simplified NTC18 approach are also reported. Discussion on the comparison between computed spectra and provision by NTC18 code are reported in the following paragraph 3, together with the other case studies.

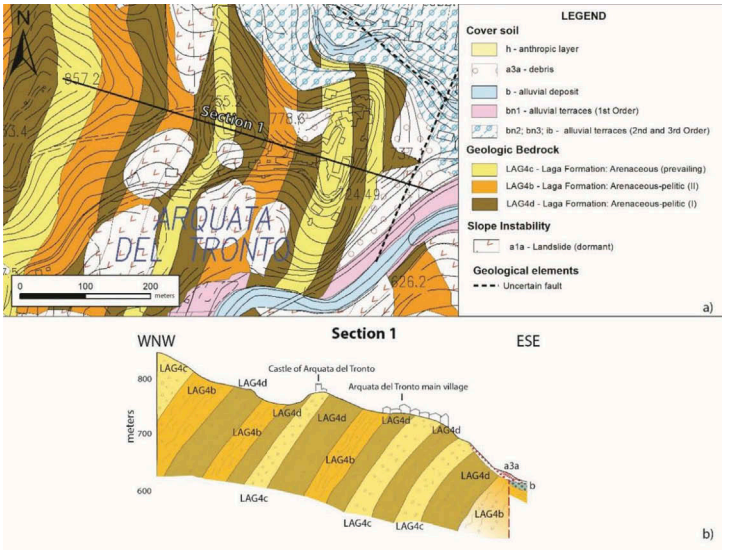

Figure 4. Lithotechnical map (a) and representative geologic cross-section 1 of the Arquata del Tronto village (b) (modified from ISPRA, 2017)

2.2 *Arquata del Tronto*

Arquata del Tronto is a municipality located in the central Apennin chain at the base of the southeastern flank of Mt. Vettore. In the study area the geological and seismic bedrock is represented by the pre-evaporitic member of the Laga Formation (e.g., Marini et al., 2016) consisting of three turbiditic lithofacies associations, largely outcropping in the study area, namely in order of increasing presence of the arenaceous component: Arenaceous-pelitic II (LAG4b), Arenaceous pelitic I (LAG4d), Arenaceous (prevailing) (LAG4c). The village of Arquata is built on an elongated WNW-ESE ridge (730 m a.s.l.) transversally cut by saddles and characterized by the alternation of stratified and roughly 50° WNW dipping different lithotypes belonging to the Laga Formation, forming a monocline representing the reverse limb of a E verging anticline. A section (Section 1) cutting Arquata del Tronto is reported in Figure 4b showing the stratigraphic relationship between different Laga Formation lithotypes.

The mechanical characterization of soils and rocks for the site response analysis has been achieved consulting the whole geological and geophysical dataset collected in the area. The geological and geophysical investigations carried out in the study area suggest the presence of a weathered/jointed upper portion of the Laga rock mass, approximately 15 meters thick. In detail, the DH test carried out on the East side of the Arquata del Tronto ridge flank, entirely located in the LAG4d lithotype, shows a V_S □ 750 m/s in the upper 15-16 m interpreted as the weathered/jointed portion of rock mass. At higher depths the V_S increases to about 1000 m/s showing no appreciable increasing trend (Pagliaroli et al., 2019a). Several HVSR tests were carried out on the Arquata del Tronto ridge, on rock outcrops belonging to different lithotypes. All the measurements highlighted the presence of multiple picks, markers of a possible broad band amplification related to coupling of stratigraphic and topography effects. An interesting observation is that the H/V curves present higher amplitude peaks if located on stiff arenaceous lithotypes of Laga Fm. as compared to those on more pelitic lithotypes of the same Formation.

The subsoil model adopted for the analyses is reported in Table 2 whereas a sketch of the mesh adopted to discretize section 1 is shown in Figure 5a. The prevalent arenaceous lithotypes of Laga Formations (LAG4c and LAG4d) were grouped together and, based on available DH tests, a Vs of 1000 m/s and 900 m/s was assigned to the arenaceous group and to the more politic lithotipe (LAG4b), respectively. As said before, a 15m-thick jointed rock-mass zone (Vs=700 m/s) was modeled at the surface of the model (Figure 5a). A Vs=1300 m/s was

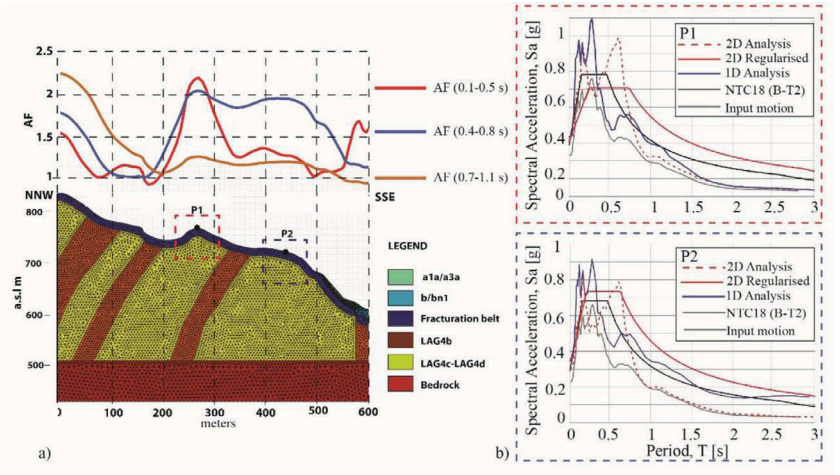

Figure 5. Arquata del Tronto site: a) mesh adopted for Section 1 and profiles of Amplification Factors (AF) computed in the three period ranges T = 0.1-0.5s, 0.4-0.8s, 0.7-1.1s; b) average acceleration response spectra at P1 and P2 computed through 2D and 1D numerical analyses compared with input and NTC18 spectrum from simplified approach.

Table 2. Arquata del Tronto site: subsoil model for site response analyses

Lithotype	γ (kN/m^3)	Vs (m/s)	ν (-)	Nonlinear material curves
a1a/a3a	19	400	0.45	Rollins et al. (1998)
b/bn1	20	500	0.43	
Jointed rock-mass	22	700	0.38	Linear D=1%
LAG4c-d	23	1000	0.4	Linear D=0.5%
LAG4b	22	900	0.4	Linear D=1%
Seismic Bedrock	24	1300	0.4	-

assumed for the bedrock considering a stiffness increment due to confining stress at depth and measurements carried out in similar geological conditions. No distinction between arenaceous and pelitic lithotipes was made for bedrock assuming that Vs values become similar at high depth. Sensitivity analyses were carried out considering different locations of seismic bedrock. For landslide/detrital cover (a1a, a3a) and alluvial (b/bn1) soils, present at the ESE ridge flank and at the toe, Vs values equal to 400 m/s and 500 m/s were assumed respectively, based on DH and MASW available tests. Regarding the nonlinear properties, literature curves for gravelly soils (Rollins et al., 1998) were employed for landslide cover and alluvial soils given the prevalent coarse grain-size composition.

The results are reported in Figure 5a in terms of amplification factors of spectral acceleration (AF) at surface computed in the three period ranges 0.1-0.5s, 0.4-0.8s and 0.7-1.1s. Major amplification effects take place in the 0.4-0.8s period range where an amplification of about 2 characterizes all the ridge, from the castle (P1 in Figure 5a) to the village (P2). In 0.1-0.5s range a peak AF=2 is attained at P1 while moderate amplification is computed at the village centre (AF=1-1.3). Finally, minor amplification effects (AF<1.2) can be observed at longer periods (0.7-1.1s). This is substantially compatible with H/V observations: the H/V curves show resonance frequencies at the ridge in the order of 1.5-5 Hz (i.e. 0.2-0.7 s) while the spectral ratios are almost flat for frequencies lower than 1.5 Hz (i.e., period > 0.7s).

In order to explore the 2D effects and physical phenomena governing the local response, additional 1D analyses were carried out at P1 and P2 using the same stratigraphic conditions of 2D simulations. The 1D acceleration response spectra averaged over the seven accelerograms are therefore compared with average 2D and input spectra in Figure 5b. Clear bi-

dimensional effects, noticed in P1 at 0.2 s and 0.6 s, are responsible for ground motion amplification in the 0.1-0.5s and 0.4-0.8s period ranges above mentioned; at P2, 1D and 2D results are much closer; however, an evident 2D effect appears at 0.6s.

Stratigraphic amplification of about 1.2-1.4 regardless the period range considered is computed at both P1 and P2 (Pagliaroli et al., 2019a). More pronounced is, therefore, the influence of the topography with 2D aggravation factors of about 2 (compare 1D and 2D spectra in Figure 5b) at selected values of period (e.g., 0.6s at both P1 and P2). In Figure 5b the regularized 2D spectra and the NTC18 spectra are also reported. See paragraph 3 for further discussion.

2.3 *Montedinove*

Montedinove is a small municipality in the southern part of the Marche region, in the Province of Ascoli Piceno, which extends for 11.9 km^2. Three different zones have been identified for the seismic microzonation: the localities of Lapedosa and Croce Rossa, severely damaged by the 2016 Central Italy Earthquake sequence, and the most densely populated historical centre.

From the morphostructural point of view, the area is characterized by a NE-SW hilly ridge, whose top reaches 561 m a.s.l. Figure 6 shows the lithotechnical map and two relevant cross-sections (BB' and CC'), which have been selected for the numerical modelling. The geological bedrock is constituted by the Blue Clays Formation which is characterized by different lithofacies: conglomeratic, arenaceous, arenaceous-pelitic and pelitic. These lithotypes, following the Italian standard for microzonation, are accordingly identified as ALS (alternation of stratified lithotypes), GRS (granular cemented substrate) and COS (cohesive, overconsolidated stratified substrate). At the ridge crest, the geological substrate is outcropping, while on the sides eluvial and colluvial coverings are present with a thickness of 3-15 m. With regards to their compositions, these soil cover deposits have been classified as GM (gravels and sandy gravels), SM (sands and silty sands) and ML (low plasticity clayey silts).

The historical centre lies mainly on GRS, locally covered by its altered upper part (SF_GRS, section CC' in Figure 6), and on ALS (section BB'). The deepest portion of the geological sequence is constituted by the upper (COS_a), the intermediate (COS_b) and the lower (COS_c) part of the cohesive, overconsolidated stratified bedrock.

The subsoil model for site response analyses was defined based on in situ geophysical and laboratory tests. Available data from the Level 1 Seismic Microzonation consist of three MASW, one P-wave SR and five HVSR tests. Additional tests were then performed in the framework of the present study to characterize all the geotechnical lithotypes. Specifically, the new survey included: 35 m deep DH test, 5 MASW tests and 24 HVSR tests. The location of the full set of investigations is reported in Figure 6. Given the lack of specific laboratory tests, nonlinear curves proposed in literature for similar materials were adopted for the lithotypes except for COSa_ and COS_b investigated by means of a RC test performed on a sample from the nearby municipality of Monte Rinaldo. Details are reported in Table 3.

The main challenge in the definition of the subsoil model was the identification of the seismic bedrock (Pagliaroli et al., 2019a). The HVSR tests carried out on the ridge crest highlighted high fundamental frequencies (10-15 Hz) consistent with the impedance contrast between the

Table 3. Montedinove site: subsoil model for site response analyses

Lithotype	γ (kN/m^3)	V_S (m/s)	ν (-)	Nonlinear material curves
SF_GRS	19.0	550	0.35	Rollins et al. (1998)
GRS	22.0	1400	0.28	Linear Viscoelastic - D = 0.5%
GM	18.6	340	0.35	Rollins et al. (1998)
SM	17.6	190	0.43	Seed and Idriss (1970)
ALS	19.6	530	0.27	Vucetic and Dobry (1991) PI=15
COS_a	19.6	560	0.46	RC Test (Monte Rinaldo)
COS_b	19.6	650	0.46	RC Test (Monte Rinaldo)
COS_c (bedrock)	19.6	800	0.46	Linear Viscoelastic - D = 0.5%

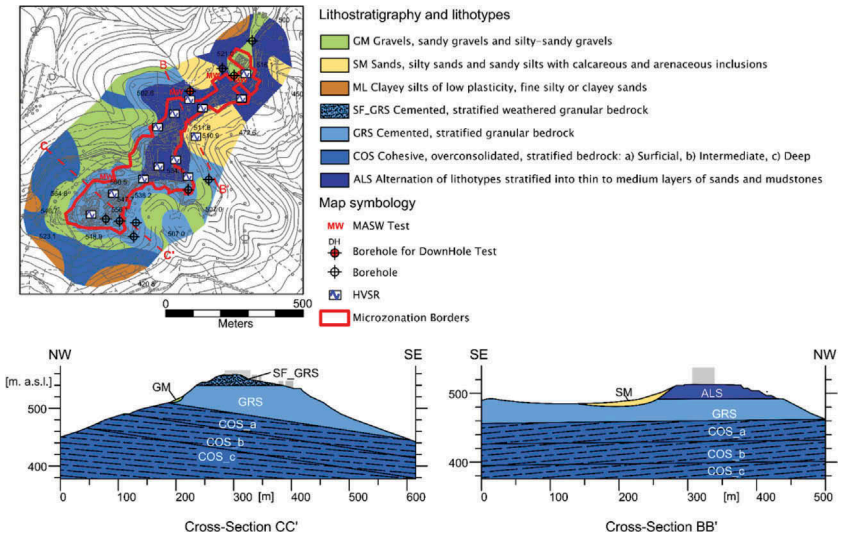

Figure 6. Montedinove site: Lithotechnical map and cross-sections of the Montedinove historical centre; lithotype codes are chosen according the Italian standards for Seismic Microzonation

SF_GRS or the ALS and the underlying GRS. Considering the high V_S value (1400 m/s) obtained by the DH test for GRS, this might lead to identifying the GRS as the seismic bedrock. However, in the whole region the GRS is underlined by COS lithotype which is characterized by medium V_S (550-650 m/s) leading to a significant shear wave velocity inversion in the subsoil. The V_S of COS increases with depth, slowly reaching values in the order of 800 m/s. This layer (COS_c in Table 3) has been therefore assumed seismic bedrock in the modelling.

The profiles of amplification factors along the surface of sections BB' and CC' are reported in Figure 7a showing that the maximum amplification effects take generally place at crest where AF=1.5-1.7 are attained regardless the period range. An exception is related to the peak due to stratigraphic amplification at SM cover along the SE flank of BB' cross-section.

In order to highlight the role of 2D effects, the results of the 2D analyses are compared in Figure 7 with the 1D simulations at the ridge crest of section BB' and CC' in terms of elastic response spectra. The results confirm the frequency-dependence of the topographic effects (2D effects take place essentially for T< 1s) and that the amount of amplification increases for steeper topographies as highlighted by previous studies (e.g. Pagliaroli et al., 2011): topographic effects are higher for steeper section CC' with respect to the gentle slope section BB'. At both sections, the 1D analyses highlight a deamplification in 0.2-0.7s range probably related to the Vs inversion between GRS and the underlying COS (Figure 7b); comparing 1D and 2D results a maximum 2D aggravation factor of about 3 is noticed for the section CC' where topographic effect takes place at 0.2-0.3s corresponding to the 2D resonance of the upper part of the ridge (above 500 m a.s.l.) constituted by GRS lithotype, as estimated by simplified formula proposed by Paolucci (2002).

2.4 *Saletta*

Saletta is a hamlet of Amatrice municipality in Lazio region, central Italy, and has been heavily struck by the 24th August 2016 Mw 6.0 experiencing a macroseismic intensity I_{EMS98} = 10. The hamlet is located on a SE-NW elongated depositional terrace composed of 10-20 m thick Pleistocene fluvial silty sands (SMtf unit in Figure 8). The SMtf unit unconformably overlies the Messinian Laga Formation, here consisting of a well bedded and gently SE-dipping sequence of lower sandstones (SFGRS unit) and upper siltstones (SFALS unit). Remnants of

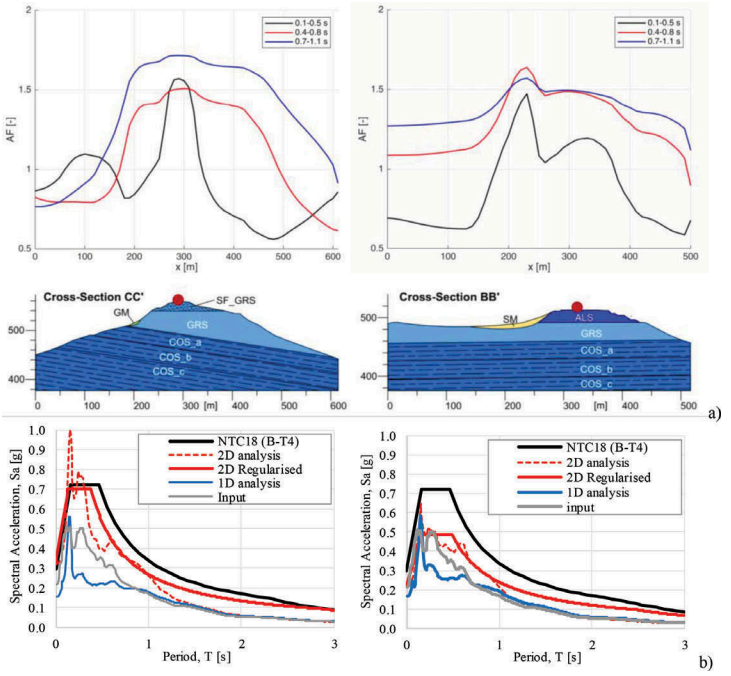

Figure 7. Montedinove site: results of the site response analyses for cross sections CC' (left) and BB' (right) in terms of a) amplification factors computed in the three period ranges T = 0.1-0.5s, 0.4-0.8s, 0.7-1.1s; b) response spectra (ξ=5%) from the 2D and 1D numerical analyses executed at the ridge crest (red points in the cross-sections) and comparison with input and NTC18 spectra.

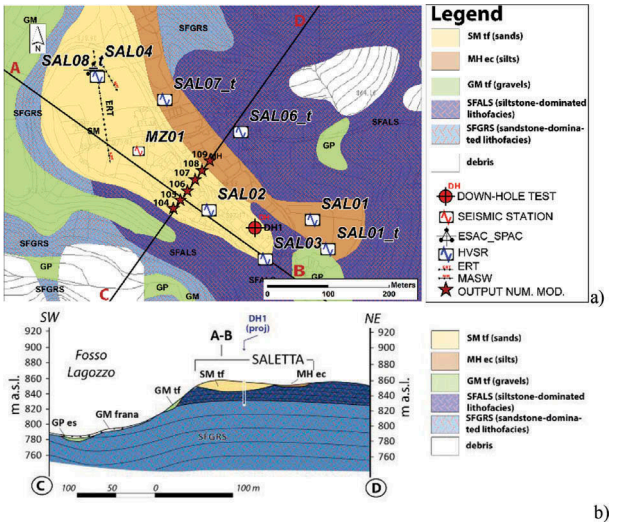

Figure 8. Saletta site: Lithotechnical map (a) and cross-sections CD (b); lithotype codes are chosen according the Italian standards for Seismic Microzonation

older and younger gravelly fluvial terraces of Quaternary age (GMtf and GPes units), each few metres thick, are found respectively up and down-slope of the sandy terrace. To NE, the Saletta terrace is partly covered by few metres of poorly consolidated colluvial silt (MHec) filling a small SE-NW trending gully, at the eastern periphery of the hamlet.

Table 4. Saletta site: subsoil model for site response analyses

Lithotype	γ (kN/m^3)	V_S (m/s)	ν (-)	Nonlinear material curves
MHec	18.0	320	0.30	«Terre rosse, L'Aquila» Amoroso et al., 2015
SMtf	18.0	320	0.30	RC test
GP, GM	20.0	450	0.40	Modoni & Gazzellone (2010)
SFALS	20.0	500	0.25	«Terre rosse, L'Aquila» Amoroso et al., 2015
SFGRS (bedrock)	22.0	800	0.25	Linear Viscoelastic - D = 0.5%

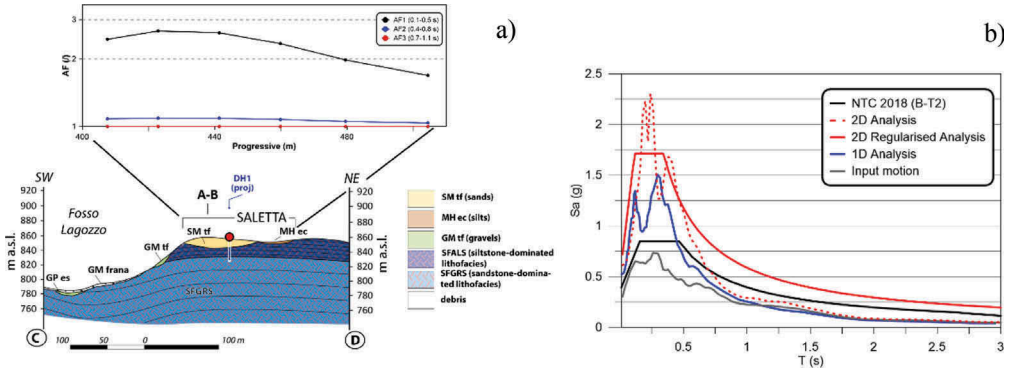

Figure 9. Saletta site: a) Amplification Factors computed in the three period ranges T = 0.1-0.5s, 0.4-0.8s, 0.7-1.1s; b) response spectra (ξ=5%) from the 2D and 1D numerical analyses executed at point #107 (see Figure 8) and comparison with input and NTC18 spectra.

The geophysical data consist of: i) an Electrical Resistivity Tomography (ERT); ii) seven noise measurements; iii) a down–hole test; iv) multichannel arrays (one acquired in active mode MASW, the other in passive mode 2D array). The geotechnical data consist of: i) a continuous 30 m deep borehole with SPT tests and ii) a resonant column (RC) test carried out on SMtf undisturbed specimen. Table 4 summarizes the main soil parameters for each unit used in 1D and 2D site response analyses.

The C-D cross-section is most significant for the study of site effects being characterized by higher amplifications with respect to A-B cross section (Gaudiosi et al., 2019). Transfer function computed from 2D analyses satisfactorily matches the amplification peak at about 5 Hz highlighted by experimental transfer function at MZ01 station (Figure 8a) thus validating the subsoil model (Gaudiosi et al., 2019). Figure 9 shows the results of the numerical analyses in terms of AFs for the cross-section C-D: the higher values, even greater than 2.5, were found for the interval of period 0.1-0.5s, with a maximum of about 3 computed close to the slope edge. This amplification can be related to stratigraphic effects associated with silty sands SMtf layer resting on stiffer SFALS/SFGRS somewhat enhanced by topographic-morphological effects. On the contrary, no significant fluctuations of AFs between 0.4-0.8s and 0.7-1.1s are observed with values lower than 1.3. Figure 9b shows the average elastic response spectra at point #107 (approximately located at DH1 projection along CD section, Figure 8) from 1D and 2D linear-equivalent analyses together with 2D regularized spectrum, input and the B-T2 spectrum according to NTC18. 1D and 2D spectra generally agree for periods higher than 0.8s while significant 2D effects take place especially in the 0.1-0.3s range where an aggravation factors of about 2 is computed; this can be ascribed to both topographic and buried morphology features.

3 STATISTICAL ANALYSIS OF AMPLIFICATION FACTORS AND COMPARISON WITH NTC18

As previously mentioned, during the Central Italy SM3 project, studies on 137 municipalities were performed. The collection of available data allows to draw some general comments. In particular, the Amplification Factors AFs, as previous defined, are analyzed in the following. A statistical distribution of the AFs (Figure 10a) has been computed with reference to all the 137 municipalities in the three period ranges Tn (with n = 1, 2, 3): $0.1 \le T_1 \le 0.5$s, $0.4 \le T_2 \le 0.8$s and $0.7 \le T_3 \le 1.1$s. A total of 4209 microzones, characterized in terms of AF by means of 1D/2D numerical analyses, were analyzed.

Median values of AF decrease from the T1 interval (where AF median value is equal to 1.5) to the T2 and T3 interval (median AF values equal to 1.3 and 1.2 respectively). For each interval of periods, most of the AF values are located close the median values, with a slightly asymmetrical distribution for T2 and T3 period ranges (Figure 10a).

For comparison, the AF values obtained as the ratio between the integral of the acceleration response spectra derived from NTC18 for the four soil classes (B-C-D-E), and the corresponding integral computed for class A were also evaluated with reference to the three ranges of periods (Figure 10b). As first approximation, topographic amplification factors have been not considered. A 475 years return period was fixed, coherently with the input motion selection for site response analyses carried out for the SM3 studies (Luzi et al. 2019). The AFs were computed for each of 137 municipalities where SM3 studies were performed at the barycentre of the principal census cell (i.e, cell which contains the municipality building) according to the Italian National Institute of Statistics (ISTAT database; https://www.istat.it/it/archivio/104317). It should be pointed out that for most microzones no equivalent shear wave velocity $V_{S,h}$ values (and therefore subsoil category classification) were generally reported in the SM3 studies. Amplification factors for each microzone were therefore computed assuming all subsoil categories of NTC18.

Comparing the results in Figures 10a and 10b, it can be observed that the NTC18 AF median values calculated for all the four soil classes are greater than the AF median values from SM3 studies in the second and third intervals of periods (medium-to-long periods). On the contrary, in the 0.1-0.5 s period range, AFs from SM3 and technical code are generally comparable: for B category the NTC18 slightly underestimate the AFs (1.3 versus 1.5) while the opposite happens for class D (1.7 vs 1.5); for C and E classes the median values of AFs are almost the same.

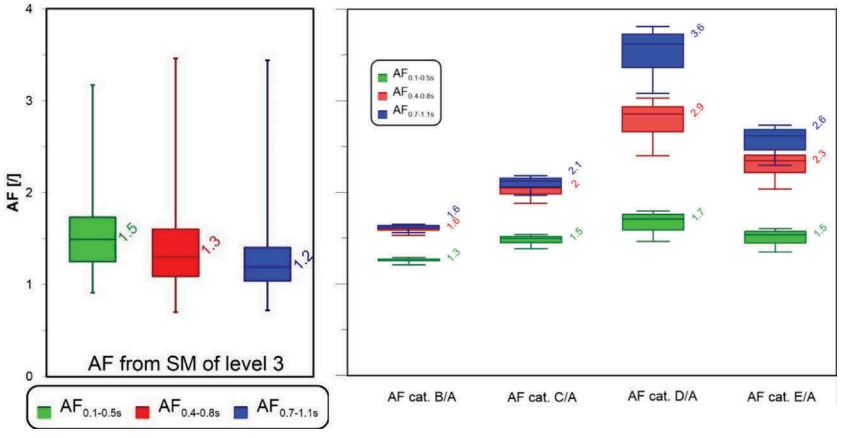

Figure 10. AF distribution for the 137 municipalities in Central Italy derived from: a) SM3 studies, b) NTC18 standard spectra for soil categories B/A, C/A, D/A and E/A; the representation uses whisker plots (minimum, 25% percentile, median, 75% percentile and maximum) with colors indicating the period range of integration (T1 is in green, T2 in red and T3 in blue) and labels referred to median values (modified from Pergalani et al., 2019).

Table 5. Comparison among AF values obtained from SM3 studies and from NTC18 spectra at the selected sites. For NTC18 the value in brackets includes the application of topographic amplification factor. In bold SM3 AFs values exceeding NTC18 factors

Site	Location	NTC18 soil-topogr. cat.	AF_{0105}		AF_{0408}		AF_{0711}	
			NTC	SM3	NTC	SM3	NTC	SM3
Monte S. Martino	V1	A – T3	1.00 (1.20)	1.15	1.00 (1.20)	**1.41**	1.00 (1.20)	**1.60**
Monte S. Martino	V2	C – T1	1.51 (1.51)	**2.23**	2.06 (2.06)	1.99	2.15 (2.15)	1.39
Monte S. Martino	V3	C – T1	1.51 (1.51)	1.41	2.06 (2.06)	**2.39**	2.15 (2.15)	1.66
Arquata del T.	P1	B – T2	1.23 (1.48)	**2.16**	1.56 (1.87)	**2.01**	1.90 (1.91)	1.19
Arquata del T.	P2	B – T2	1.23 (1.48)	1.23	1.56 (1.87)	1.87	1.90 (1.91)	1.19
Montedinove	BB'- crest	B – T4	1.27 (1.78)	1.20	1.61 (2.25)	1.48	1.64 (2.30)	1.46
Montedinove	CC'– crest	B – T4	1.27 (1.78)	1.57	1.61 (2.25)	1.51	1.64 (2.30)	1.72
Saletta	CD – crest	B – T2	1.22 (1.46)	**2.66**	1.55 (1.86)	1.09	1.57 (1.88)	1.00

In order to compare NTC18 and SM3 AFs with reference to the same soil category, a comparison was undertaken for the four sites presented in the previous section. In Table 5 for different points of the four sites, the corresponding subsoil and topographic NTC18 categories were identified. AFs from SM3 spectra obtained from 2D analyses and presented in the previous sections were computed. For NTC18 two values of AFs were calculated: one considering only the stratigraphic amplification (i.e., using the standard spectra pertaining to the reference subsoil category) and another one (in brackets) by considering also the topographic amplification (i.e, using also the topographic category).

In the T1 and T2 period ranges (0.1-0.5s, 0.4-0.8s), AFs from NTC18 in most cases are comparable or higher than SM3. There are some exceptions, in which NTC18 is non-conservative because 2D effects are very relevant: pure topographic effects (Monte San Martino V1, Montedinove CC' crest), complex phenomena related to the coupling of stratigraphic and topographic effects (Saletta) or coupling of topographic and jointed rock mass effects (Arquata), buried morphology effects (Monte San Martino V2). In these cases, the underestimation of amplification factors by NTC18 is due to: i) inability of NTC18 spectra essentially based on 1D stratigraphic effects to capture buried morphology effects, ii) inadequacy of code frequency independent topographic factors which underestimate spectral peak of topographic amplification (see Monte San Martino V1 and case studies collected in Pagliaroli et al., 2011).

In T3 period range, AFs from NTC18 are largely conservative with respect to SM3 amplifications thus confirming what observed in Figure 10 for all the municipalities even if no D and E categories are present in the four analyzed cases. The severe overestimation of the AFs in the medium-to-high period range (0.7-1.1s) by the Italian technical code could be probably ascribed to the inadequacy of soil factors Cc controlling the shape of the spectra by enlarging the plateau at higher periods with respect to rock conditions (Aimar et al., 2018; Pagliaroli et al., 2019b). More research is necessary to ascertain the causes of divergence between SM3 and NTC18 amplification factors; in particular, AF comparisons undertaken separately for each subsoil category could significantly improve the analysis.

4 APPLICATIONS OF SM STUDIES IN SUPPORTING SEISMIC DESIGN

Appropriate actions can be undertaken in order to mitigate seismic risk and reduce it below an acceptable level. This can essentially be done: i) at the building scale by means of the adoption of up-to-date building codes (e.g., NTC18) and seismic retrofitting programs, ii) at the urban scale by means of SM studies and their inclusion in urban/territory planning tools. These tools for seismic risk mitigation, namely technical code and SM, operate with different objectives and at different scales; however, as both require the quantitative assessment of local seismic hazard (site effects), some ambiguity in the definition of the boundaries between SM3

and NTC18 and on the possible use of SM3 output in the seismic design still exist. The outcome of SM3 studies are undoubtedly useful for the design as (Pagliaroli, 2018):

- provide a large database of subsoil investigations allowing: i) to be more aware in planning the investigation survey at the building scale, ii) to access large scale investigations, the cost of which is generally unsustainable at least for ordinary design (e.g., geophysical investigations for the identification of deep buried morphologies and/or deep seismic bedrock);
- alert the designer on possible instability phenomena; in this case the designer should perform additional subsoil investigations and quantitative stability analyses depending on the design phase and type of instability phenomenon (liquefaction, slope instability, cavity collapse);
- provide objective indications on which approach is more appropriate for the evaluation of the seismic action (e.g., code simplified approach based on subsoil categories or *ad hoc* site response numerical analyses).

Regarding this last issue, following the SM3 studies in the municipalities of Central Italy, general criteria for the use of the results of these studies in the reconstruction process were proposed in the "Ordinanza n. 55/2018" (Presidency of the Council of Ministers, 2018). In order to define the design spectrum, the designer must preliminary compare the spectrum derived from the SM3 studies (regularized according to the procedure proposed in Working Group ICMS 2008) with the spectrum from the NTC18 simplified approach. If the SM3 spectrum exceeds punctually 30% the NTC18 spectral values or the integral of the SM3 spectrum in the period range of interest exceeds 20% the NTC18 one, the simplified NTC08 approach can be regarded as non-conservative. In this case, the designer should perform additional investigations in the significant subsoil volume and is strongly encouraged to perform site response analyses to define the seismic action. Moreover, in case of complex surficial or buried morphologies, the designer should consider the direct use of the SM3 spectra for the design provided that these actions derived from 2D SM3 analyses are considered more accurate than site response analyses usually performed with standard 1D methods at building scale in the design process.

5 CONCLUSIONS

Seismic Microzonation studies based on numerical simulations of site response were carried out for the reconstruction of 137 municipalities in Central Italy struck by the 2016 seismic sequence. The paper presents the main results of 1D/2D site response numerical analyses at 4 selected sites characterized by complex morphological and geological conditions (Monte San Martino, Arquata del Tronto, Montedinove and Saletta). Results are presented in terms of amplification factors in three selected period ranges 0.1-0.5, 0.4-0.8 and 0.7-1.1s (to be used in setting the SM3 maps) and response spectra at relevant points (to be associated to the microzones of SM3 maps). The comparison between 1D and 2D response spectra allowed to highlight 2D effects computing 2D aggravation factors. Moreover, computed amplification factors were compared to the corresponding parameters derived from the Italian technical code NTC18. Relevant amplification effects take place at specific points of the investigated areas: pure topographic effects at San Martino and Montedinove crests, complex phenomena related to the coupling of stratigraphic and topographic effects (Saletta crest), coupling of topographic and jointed rock mass effects (Arquata crest), effects of buried morphology at the edge of covers (Monte San Martino slope). In these cases, 2D aggravation factors, comprised between 2 and 3, affect essentially the first two period ranges (0.1-0.5s and 0.4-0.8s). In these points amplification predicted by NTC18 is non-conservative due to: i) inability of NTC18 spectra essentially based on 1D stratigraphic effects to capture buried morphology effects, ii) inadequacy of code frequency independent topographic factors. In most cases, i.e., in areas where 2D effects are less important, NTC18 provisions lead to amplifications comparable or higher than those computed by site response analyses. At high periods (third range 0.7-1.1s) NTC18 is overconservative probably for the inadequacy of spectral shapes. This is confirmed by a simplified and preliminary statistical

analysis carried out considering amplifications factors computed for all 137 municipalities subjected to SM3 studies and compared with NTC18.

Finally, following the "Ordinanza n. 55/2018" (Presidency of the Council of Ministers, 2018), some proposal on the possible use of SM3 outputs in supporting seismic design are reported. In particular, the response spectra produced in the SM3 studies, compared with NTC18 spectra, provide objective indications on the most suitable approach for the evaluation of the seismic action (e.g., technical code simplified approach based on subsoil categories or *ad hoc* site response numerical analyses).

REFERENCES

Aimar, M., Ciancimino, A. & Foti, S. 2018. Valutazione dei metodi semplificati proposti nelle NTC18 per la stima degli effetti di sito: un approccio stocastico. *Proc. IARG 2018*

Amoroso, S., Totani, F., Totani, G. & Monaco, P. 2015. Local seismic response in the Southern part of the historic centre of L'Aquila. In: Springer International Publishing (ed) *Eng. Geol. for Society and Territory—Urban Geology, Sustainable Planning and Landscape Exploitation*5(XVIII):1097–1100.

Caielli, G., de Franco, R., Di Fiore, V., Albarello, D., Catalano, S., et al. 2019. Extensive surface geophysical prospecting for seismic microzonation. *Bulletin of Earthquake Engineering* (under review).

CEN (European Committee for Standardization) 2004. Eurocode 8: Design of structures for earthquake resistance, Part 1: general rules, seismic actions and rules for buildings. EN1998–1:2004, Brussels.

Chiaraluce, L., Di Stefano, R., Tinti, E., Scognamiglio, L., Michele, M., Casarotti, E., Cattaneo, M., De Gori, P., Chiarabba, C., Monachesi, G., Lombardi, A. M., Valoroso, L., Latorre, D. & Marzorati, S. 2017. The 2016 Central Italy seismic sequence: a first look at the mainshocks, aftershocks and source models. *Seism. Res. Lett*., 88 (3), 1-15, doi:10.1785/0220160221.

Ciancimino, A., Foti, S., Alleanza, G. A., Amoroso, S., Bardotti, R. et al. 2019. Dynamic characterization of soils in Central Italy through laboratory testing. *Bulletin of Earthquake Engineering* (under review).

Gaudiosi I., Vignaroli G., Mancini M., Moscatelli M., Simionato M. et al. 2019. Site effects in Saletta damaged area of Amatrice municipality (Central Italy) after the 24th August 2016 earthquake. *Proc. 7th Int. Conf. on Earthquake Geotechnical Engineering (ICEGE)*, Roma, June 2019 (submitted).

Hashash, Y. Musgrove, M. Harmon J. Groholski D. Phillips C. & Park D. 2016. DEEPSOIL 6.1, User Manual. Urbana, IL: Board of Trustees of University of Illinois at Urbana-Champaign.

Hudson, M. Idriss, I. & Beikae, M. 1994. User's Manual for QUAD4M. Center for Geotechnical Modeling, Department of Civil & Environmental Engineering, University of California, Davis, California.

ISPRA 2017. Attività propedeutiche alla Microzonazione Sismica nell'area del comune di Arquata del Tronto (AP). Report (in italian)

Kottke, A. R., Wang, X. & Rathje, E. M. 2013. Technical Manual for Strata. Geotechnical Engineering Center, Dep. of Civil, Architectural, and Environmental Engineering, University of Texas, 89 pp.

Lanzo G., Pagliaroli A. & D'Elia B. (2003). Numerical study on the frequency-dependent viscous damping in dynamic response analyses of ground. In: Latini & Brebbia (eds), *Earthquake Resistant Engineering Structures IV*, WIT Press, Southampton, Boston, pp. 315-324.

Luzi, L., Pacor, F., Felicetta, C., Puglia, R., Lanzano, G. & D'Amico, M. 2019. 2016-2017 Central Italy seismic sequence: strong-motion data, seismic hazard and design earthquake for the seismic microzonation of Central Italy. *Bulletin of Earthquake Engineering* (under review).

Madiai C., Facciorusso J. & Gargini E., 2017. Numerical modeling of seismic site effects in a shallow alluvial basin of the Northern Apennines (Italy). *Bull. Seism. Society America*, 107(5), pp. 2094-2105.

Marini, M., Felletti, F., Milli, S. & Patacci, M. 2016. The thick-bedded tail of turbidite thickness distribution as a proxy for flow confinement: Examples from tertiary basins of central and northern Apennines (Italy). *Sedimentary Geology*, 341, 96-11

Ministry of Infrastructure and Transportation 2018. D.M. 17/01/2018. Aggiornamento delle «Norme Tecniche per le Costruzioni». Gazzetta Ufficiale, n.42 del 20/ 02/2018– supplemento ordinario n.8.

Modoni, G. & Gazzellone, A. 2010. Simplified theoretical analysis of the seismic response of artificially compacted gravels. V International Conference on Recent Advances in Geotechnical Earthquake Engineering and Soil Dynamics, Paper No. 1.28a. San Diego (USA).

Pagliaroli, A.& D'Elia, B. 2011 Numerical evaluation of topographic effects at the Nicastro ridge in Southern Italy. *Journal of Earthquake Engineering*, 15(3),404-432.

Paolucci, R. 2002. Amplification of earthquake ground motion by steep topographic irregularities. *Earthquake Engineering and Structural Dynamics* 31, 1831–1853.

Pagliaroli A. 2018. Key issues in Seismic Microzonation studies: lessons from recent experiences in Italy. *Italian Geotechnical Journal*, 1/2018, 5-48,

Pagliaroli, A, Pergalani, F., Ciancimino, A., Chiaradonna, A., Compagnoni, M. et al. 2019a. Site response analyses for complex geological and morphological conditions: relevant case-histories from 3rd level seismic microzonation in Central Italy. *Bulletin of Earthquake Engineering* (under review).

Pagliaroli A., Papa V. & Pisotta I. 2019b. Stratigraphic amplification factors based on KiK-net downhole recordings and parametric 1D site response analyses: evaluation and comparison with code provisions. Proc. 7th Int. Conf. on Earthquake Geotechnical Engineering (ICEGE), Roma, June 2019 (submitted).

Pergalani, F., Bordeaux, G., Compagnoni, M., Gaudiosi, I., Lenti, L. et al. (2019). Seismic microzoning map: approaches, results and applications after the 2016-2017 Central Italy seismic sequence. *Bulletin of Earthquake Engineering* (under review).

Pitilakis, K., E. Riga, A. Anastasiadis & K. Makra 2015. New elastic spectra, site amplification factors and aggravation factors for complex subsurface geometry towards the improvement of EC8, 6th International Conference on Earthquake Geotechnical Engineering, Christchurch, New Zealand.

Presidency of the Council of Ministers (2018). Ordinance 55 del 24/ 04/2018. Available at: https://sisma2016.gov.it/2018/04/24/ordinanza-n-55-registrata-il-24-aprile-2018-al-n-846/, last accessed January 2019 (in italian).

Rollins, K. M., Evans, M. D., Diehl, N. B. & Daily III, W. D. 1998. Shear modulus and damping relationships for gravels. *Journal of Geotechnical and Geoenvironmental Engineering*, 124(5): 396-405.

Seed H.B., Idriss I.M. 1970. Soil moduli and damping factors for dynamic response analyses. *Technical Report EERRC-70-10, University of California, Berkeley*.

STACEC srl 2017. LSR 2d (Local Seismic Response 2d), http://www.stacec.com.

Vucetic, M. & Dobry, R. 1991. Effects of the soil plasticity on cyclic response. *J. Geot. Eng. Div*. 117, 89-107.

Working Group ICMS 2008. Indirizzi e criteri per la microzonazione sismica – Guidelines for seismic microzonation. Conferenza delle Regioni e delle Province Autonome-Dip. della Protezione Civile.